Thermochimica Acta, 241 (1994) 247–258
Elsevier Science B.V., Amsterdam
SSDI 0040-6031(93)01667-R

A kinetic study of the chlorination of MO_3 by CCl_4

I.S. Pap [a], G. Mink [a,*], A. Auroux [b] and E. Karmazsin [c]

[a] *Research Laboratory for Inorganic Chemistry, Hungarian Academy of Sciences, P.O.B. 132 H-1502, Budapest, Hungary*
[b] *Institute de Recherches sur la Catalyse, CNRS, 2. Avenue Einstein, 69626 Villeurbanne, France*
[c] *Claude Bernard University, Department of Applied Chemistry, Lyon, France*

(Received 2 June 1993; accepted 11 December 1993)

Abstract

The surface and morphological properties of molybdenum trioxide were characterized using microcalorimetric and SEM methods. The number of acidic and basic sites were measured by NH_3 and SO_2 adsorption, respectively. According to the microcalorimetric data, strong dissociative adsorption of NH_3 takes place on the surface, while there is no interaction between the MO_3 lattice and SO_2 gas.

The chlorination kinetics of MO_3 with gaseous CCl_4 were studied by thermogravimetry. The values of the apparent activation energy and the formal reaction order were calculated from the temperature and partial pressure dependence of the initial rate, respectively. From the results obtained, the combined control of pore diffusion and chemical reaction, as well as the dissociative adsorption of CCl_4, were deduced.

Due to the very low porosity of the solid particles, in addition to the reaction occurring in a zone near the pore tunnels, chlorination at the external surface cannot be neglected. Thus, to describe the conversion versus time curves, a kinetic model was proposed based on the different linear rates of the interfacial chemical reaction at the external surface of the particles and that in the reaction zone controlled by pore-diffusion processes. Using this model, a fairly good correspondence between the measured and calculated kinetic curves was obtained.

INTRODUCTION

In heterogeneous gas–solid reactions, the surface structure and phase composition have a great influence on the reaction rate. Morphological changes during the reaction may significantly affect the kinetics, especially in cases when transport processes play a rate-controlling role. The present paper reports a detailed kinetic investigation of a simple gasification reaction for cases when the solid sample has a relatively low specific surface area.

* Corresponding author.

Molybdenum oxides have a high reactivity towards the various chlorinating agents [1]. Various preparation routes for the different Mo-chlorides and oxychlorides have been investigated extensively [2–6]. Much less attention has been paid to the kinetics of the reactions with gaseous chlorinating agents [7–9].

In the present work, the volatilization of MoO_3 of low specific surface area with gaseous CCl_4 was chosen as the model reaction. A kinetic model is proposed to interpret the anomalous shape of the conversion versus time curves. In order to explain the high reactivity of molybdenum oxide, the nature and number of the surface active sites were also investigated.

EXPERIMENTAL

Thermogravimetric measurements were carried out in a special reactor attached to a Mettler semi-micro recording balance.

Powder-like molybdenum trioxide of analytical grade (Reanal) was used. The crystalline structure of the sample was checked by X-ray diffraction analysis. Before the chlorination the samples were preheated in situ at 773 K for 30 min in an O_2–N_2 mixture. A large excess of inlet-active gas was used to maintain conditions in the differential-type flow reactor.

The chlorinating agent was reagent grade CCl_4, which was introduced from a bubbler. Nitrogen of 4N purity, dried in the usual manner, was used as inert diluting gas.

The surface properties of the solid sample was investigated by a microcalorimetric method. NH_3 and SO_2 were used for measuring the acidic and basic sites. The adsorption of the reactive gases was performed at 353 K in order to avoid physisorption. The heats of adsorption were determined in a differential heat-flow calorimeter (Setaram) linked to a volumetric line, which permitted the introduction of successive small pulses of the reactive gases. The experimental set-up has been described elsewhere [10]. In order to homogenize the phase, all the samples were outgassed at 573 K for 3 h before the calorimetric experiments.

The morphology of the MO_3 samples was characterized by SEM measurements. The specific surface areas of the initial samples and the chlorinated residues were determined by O_2 adsorption at 77 K by the usual BET method.

RESULTS AND DISCUSSION

Thermochemical calculations

Thermochemical calculations for some of the possible main and side reactions were made for the temperature range 300–1000 K, using the data published in the JANAF tables [11] and in ref. 12. The temperature

TABLE 1

Equilibrium constants for reactions (1–8)

T/K	log K_p							
	(1)	(2)	(3)	(4)	(5)	(6)	(7)	(8)
300	17.450	14.305	34.468	40.919	17.018	23.469	−5.521	−8.291
400	15.827	13.751	30.691	34.420	14.865	18.593	−2.138	−4.349
500	14.811	13.369	28.371	30.479	13.560	15.669	−0.220	−2.072
600	14.103	13.079	26.780	27.818	12.677	13.715	0.970	−0.676
700	13.575	12.848	25.607	25.888	12.032	12.313	1.744	0.371
800	13.158	12.651	24.698	24.416	11.540	11.258	2.261	1.071
900	12.819	12.481	23.968	23.253	11.149	10.434	2.610	1.577
1000	12.532	12.328	23.361	22.303	10.829	9.771	2.844	1.950

$MoO_3(s) + 0.5CCl_4(g) = MoO_2Cl_2(g) + 0.5CO_2(g)$ (1)

$MoO_3(s) + CCl_4(g) = MoO_2Cl_2(g) + COCl_2(g)$ (2)

$MoO_3(s) + 1.5CCl_4(g) = MoCl_4(g) + 1.5CO_2(g) + Cl_2(g)$ (3)

$MoO_3(s) + 1.5CCl_4(g) = MoCl_5(g) + 1.5CO_2(g) + 0.5Cl_2(g)$ (4)

$MoO_2Cl_2(g) + CCl_4(g) = MoCl_4(g) + CO_2(g) + Cl_2(g)$ (5)

$MoO_2Cl_2(g) + CCl_4(g) = MoCl_5(g) + CO_2(g) + 0.5Cl_2(g)$ (6)

$MoCl_4(s) = MoCl_4(g)$ (7)

$MoCl_5(s) = MoCl_5(g)$ (8)

dependences of the equilibrium constants for reactions (1)–(6) are given in Table 1. As can be seen, the chlorination reactions, resulting in Mo chloride and oxychloride, are highly favoured. The Mo chlorides are volatile in the temperature range of the kinetic measurements (processes (7) and (8)). It is also known that MoO_2Cl_2 undergoes sublimation at higher temperatures [11]. In accordance with this expectation, only crystalline MoO_3 was detected by XRD in the chlorinated residue.

Similar results were published recently by Del Carmen Ruis [9] during the investigation of $MoO_3 + CCl_4$ at 713–733 K. According to these data, the chlorination products are mostly $MoO_2Cl_2(g)$, $CO_2(g)$, $Cl_2(g)$ and $COCl_2(g)$. Thus, the chlorination can be described by processes (1) and (2). The reaction products are volatile, and the kinetics of the reaction can be followed by thermogravimetry.

Morphological and calorimetric characterization of the MO_3 sample

Molybdenum oxides (except $Mo_{17}O_{47}$) have been described as "tunnel compounds" [1] because they contain wide empty tunnels that pass through their structures. Molybdenum(VI) oxide is known to be orthorhombic. The oxide phase has a layer structure consisting of parallel rows of distorted MoO_6 octahedra [13].

TABLE 2

Acid–base properties of MoO_3

	Number of active sites in μmol m^2	Heat of adsorption in kJ mol^{-1}	
		Average	Initial
Acidic sites (NH_3 ads.)	7.2	16.8	119.9
Basic sites (SO_2 ads.)	0		
Surface Mo ions [a]	14.2		

[a] Calculated from the crystal structure of MoO_3 according to ref. 1.

According to the BET data the sample used can be characterized by a relatively low specific surface area of 3.5 m^2 g^{-1}. As shown by SEM examination of the sample, the shape of the MO_3 particles can be considered as nearly cylindrical polyhedrons. From the SEM images, an average diameter of 0.7 μm can be deduced. Assuming non-porous particles, this value corresponds to an external surface area of only 1.8m^2 g^{-1}. Thus, we assume that the cylindrical polyhedrons have a low but not negligible inner porosity with an additive inner surface area.

On the basis of the TD calculations and the BET data and SEM and XRD measurements, the process investigated can be categorized as gasification reactions of porous solids.

The acidic and basic features of the MO_3 surface were characterized by a volumetric–microcalorimetric method. The number of acidic and basic sites measured by NH_3 and SO_2 adsorption, as well as the average heat of adsorption, are given in Table 2. As can be seen, MoO_3 as an acidic oxide, vigorously adsorbs NH_3. While there is no detectable adsorption of SO_2. The population of the surface Mo ions, calculated from the crystal structure of molybdenum trioxide [1], is also given in Table 2. According to the data, the number of acidic sites is practially half the total number of surface Mo ions. Thus, dissociative adsorption of NH_3 molecules on the Mo–O–Mo–O– sites can be assumed with the formation of surface Mo–NH_2 and Mo–OH species. This type of adsorption takes place on the total surface area, and monolayer coverage is easily achieved.

Kinetics of the chlorination reaction

The reaction kinetics were followed by isothermal thermogravimetric measurements in the temperature range 580–750 K at 2–12 kPa CCl_4.

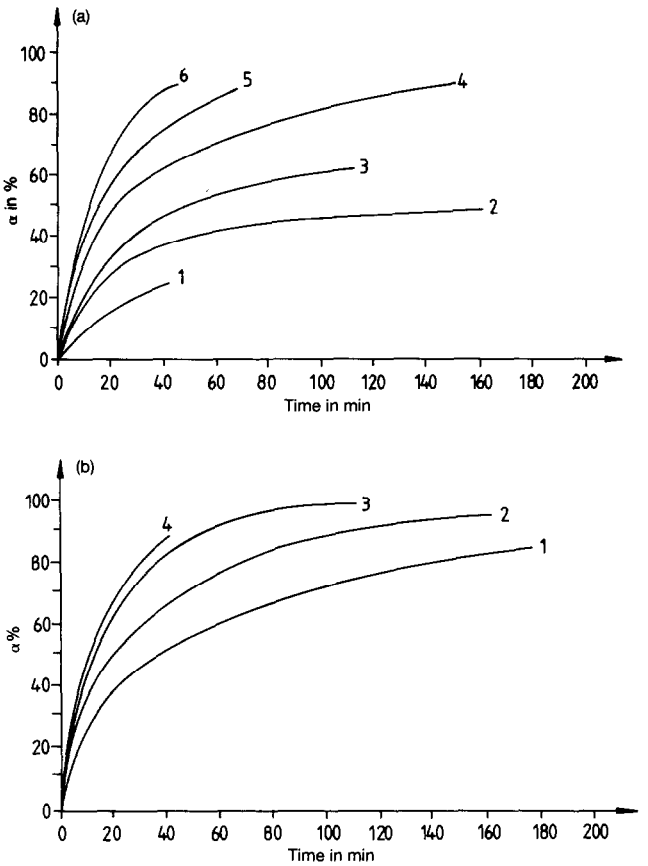

Fig. 1. Conversion versus time curves. a. p = 10.1 kPa CCl_4: curve 1, 580 K; curve 2, 620 K; curve 3, 650 K; curve 4, 680 K; curve 5, 700 K; curve 6, 740 K. b. $T = 740$ K: curve 1, 2.5 kPa; curve 2, 5.0 kPa; curve 3, 7.6 kPa; curve 4, 10.1 kPa CCl_4.

Some characteristic conversion (relative mass loss) versus time curves are shown in Figs. 1a and 1b. As can be seen, no mass gain relating to formation of solid reaction products was observed, even at the beginning of the chlorination process. The reaction starts with a continuous mass loss due to the volatilization of the gaseous products. The initial reaction rate R_0 was determined as the initial slope of the mass loss versus time curves related to unit mass.

The partial pressure dependence of the reaction was studied in the range of 2–12 kPa CCl_4. The formal orders were calculated from the logarithmic representation of the initial rates. According to the data, reaction orders of $n = 0.75$ and $n = 0.5$ were found at 680–750 K and at 590 K, respectively. As a consequence, linear R_0 versus $p^{3/4}$ and R_0 versus $p^{1/2}$ plots were obtained, as shown in Figs. 2a and 2b.

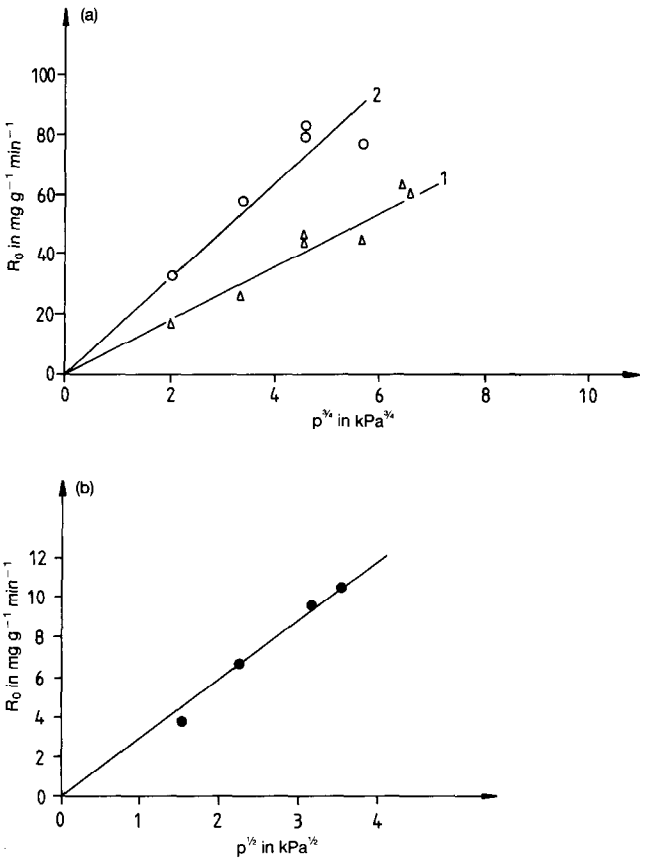

Fig. 2. a. R_0 vs. $p^{3/4}$ functions for the chlorination by CCl_4: curve 1, 680 K; curve 2, 740 K. b. R_0 vs. $p^{1/2}$ functions for the chlorination by CCl_4, $T = 590$ K.

The Arrhenius representation of the initial reaction rates is shown in Fig. 3. According to the data, activation energies of 110 and 53 kJ mol^{-1} were obtained in the temperature ranges 550–600 and 600–700 K, respectively. As can be seen, the apparent activation energy in the higher temperature range is about half of that determined below 600 K. This suggests that at low temperatures the reaction is controlled by the chemical process, while above 600 K the reaction changes to the pore-diffusion-controlled process.

This assumption is also supported by the variation of the specific surface area during the reaction at 670 K, shown in Fig. 4. As known, for the gasification of non-porous solids, the specific surface area increases monotonously during the reaction. SEM and BET data suggest that the MoO_3 studied has inner porosity. Above 600 K, pore-diffusion control is thought to explain the kinetic data. Figure 4 shows that the specific surface area barely changes during the chlorination: only a slight decrease, then a moderate increase, can be observed during the volatilization. This suggests

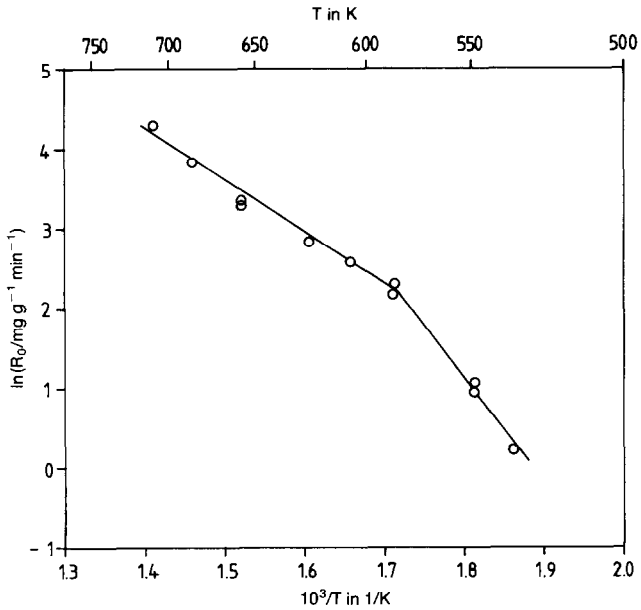

Fig. 3. Arrhenius representation of the initial reaction rates R_0.

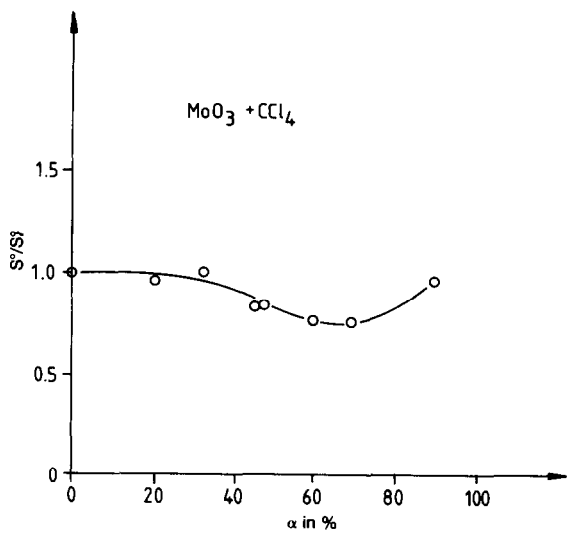

Fig. 4. Variation of the specific surface area during the chlorination, $T = 670$ K; where S_i^0 is the initial value at zero conversion.

that the reaction takes place at the pore walls in a reaction zone near to the external surface, while the centre of the pellets remains relatively unchanged until the final stages of the reaction.

Considering the geometric structure of CCl_4, the homogen (gas phase) or surface dissociation of CCl_4 must precede the chlorination reaction. In

our cases, the gas-phase decomposition of CCl_4 can be neglected. It was detected in the same equipment by separate thermogravimetric–mass-spectrometric measurements [13]. Thus the surface dissociation must be taken into account during the chlorination. On the basis of the above kinetic considerations, the reversible dissociative adsorption of CCl_4 precedes the volatilization, resulting in a low coverage of the adsorbed CCl_3^* and Cl^* radicals, with reaction orders of $n = 0.5$ and $n = 0.75$ in the chemically controlled region and at temperatures where the transport processes play the rate-controlling role, respectively. Thus the characteristic partial-pressure dependence of the initial rates shown in Figs. 2a and 2b can be explained by assuming the surface dissociation of CCl_4.

In the first step of the chlorination, the adsorbed CCl_3^* radicals react with the lattice oxygen resulting in a surface oxygen–chlorine exchange

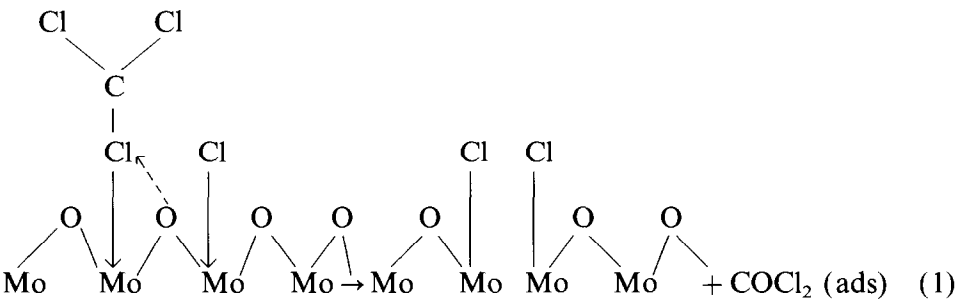

(1)

Because this chlorine-substituted surface is the intermediate product of the reaction, it could not cause layer-diffusion limitation. In the second step, the chlorine-substituted surface reacts with the active gas and volatile $MoO_2Cl_2(g)$ is formed.

In order to describe the conversion versus time curves, various kinetic models [15], based on the equation $-d\alpha/dt = kf(\alpha)$, were tested. According to these calculations, neither the simple model of contracting cylindrical particles nor other commonly used kinetic models could be applied for describing the conversion–time data.

As detected by the morphological examinations, the inner porosity of the MO_3 particles is very low but not negligible. In this case, the reaction on the external surface area may be significant as compared to the reaction at the internal pore walls [16]. As a consequence, the rate is different in the reaction zone near the pore tunnels and at the external surface. Therefore, a kinetic model is suggested for describing the shape of the conversion–time curves, as follows.

Contracting cylinder model for particles with very low porosity

The proposed model is based on the following assumptions:

(i) The reaction proceeds along a coordinate perpendicular to the surface by a linear function of the time ($-dr/dt = \text{const.}$).

(ii) The particles are very close to being cylindrical in shape with uniform radii ($^{\circ}R \equiv 1$ in arbitrary units). The reaction on the bases is neglected compared to that on the surface of the cylinder.

(iii) Due to the layer structure of MO_3, the pore tunnels are parallel to each other and perpendicular to the surface.

In this case the rate of interfacial chemical reaction on the non-porous surface [17] can be expressed by

$$-\frac{dr}{dt} = \frac{kfc^n}{\rho} = k_1 \tag{2}$$

where k is the rate constant of the chemical process, f is the roughness factor for the external surface, c is the concentration of the gaseous reactant, n is the reaction order and ρ is the molar density of the solid phase. By integrating eqn. (2) from $r = {}^{\circ}R \equiv 1$ to r, where r is some value between 0 and 1

$$r = {}^{\circ}R - k_1 t = 1 - k_1 t \tag{3}$$

The reaction rate at the pores [16] in a reaction zone of thickness z for particles of low porosity can be expressed

$$-\frac{dr}{dt} = \frac{[2kS_v D_e/(n+1)]^{1/2} c^{(n+1)/2} + kfc^n}{\rho} = k_2 \tag{4}$$

where S_v is the surface area per unit volume of the pellet and D_e is the effective diffusivity of the gaseous reactant in the pores. After integration of eqn. (4)

$$r = {}^{\circ}R - k_2 t = 1 - k_2 t \tag{5}$$

From eqns. (3) and (5), the fraction of the unreacted solid mass can be expressed as

$$\frac{m}{m_0} = \frac{(1-k_1 t)^2 \pi (1 - \Sigma z)\rho + (1-k_2 t)^2 \pi (\Sigma z)\rho}{{}^{\circ}R^2 \pi l \rho} \tag{6}$$

It is apparent from eqns. (2) and (4), that $k_2 > k_1$, i.e. the reaction rate is higher surrounding the pores than on the non-porous surface.

Thus the conversion–time curves can be calculated by the following equations: if $k_2 t < 1$

$$\alpha = 1 - m/m_0 = 1 - [(1-q)(1-k_1 t)^2 + q(1-k_2 t)^2] \tag{7}$$

If $k_2 t \geq 1$.

$$\alpha = 1 - m/m_0 = 1 - [(1-q)(1-k_1 t)^2] \tag{8}$$

where $q = (\Sigma z)/l$ is the ratio of the total thickness of the reaction zone controlled by the pore diffusion to the whole length of the cylindrical particles 1.

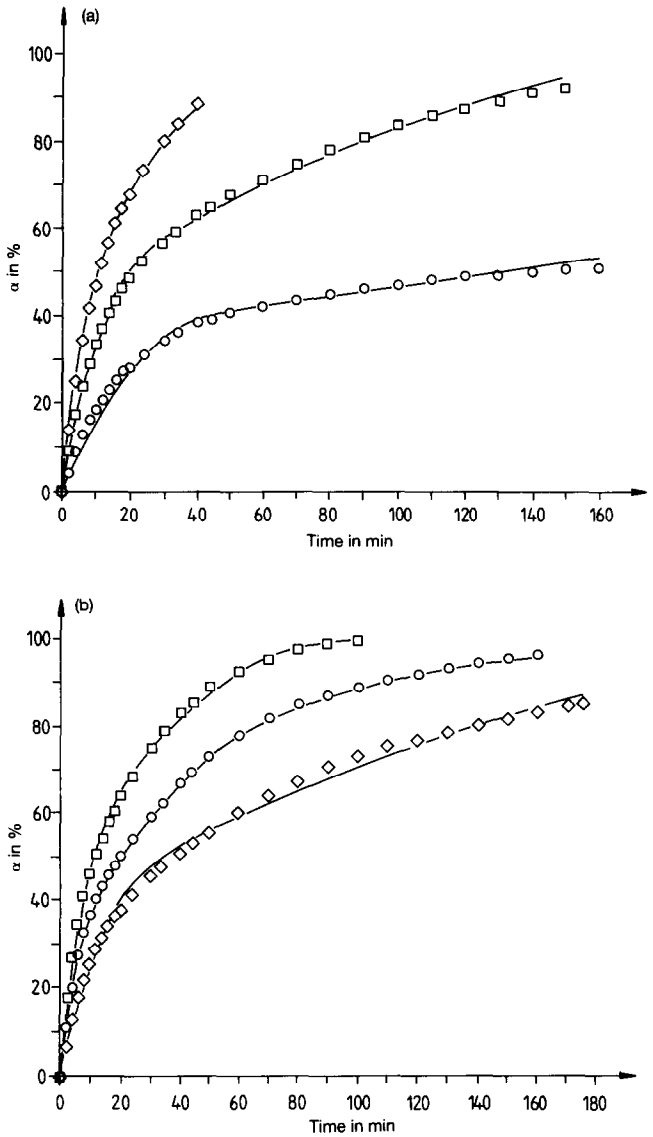

Fig. 5. Calculated and observed conversion vs. time curves. a. $p = 10.1$ kPa CCl_4: ○, 620 K; □, 680 K; ◇, 750 K. b. $T = 740$ K: ◇, 2.5 kPa; ○, 5.0 kPa; □, 7.5 kPa CCl_4.

The ratios of k_1/k_2 and q should be regarded as interpolation variables.

Figures 5a and 5b show the conversion–time data, measured at different temperatures and partial pressures, as well as the curves calculated using the proposed kinetic model. The suitable k_1/k_2 and q values varied between 0.05 and 0.2 and between 0.53 and 0.66, respectively. As can be seen, a fairly good correspondence between the measured and calculated curves was obtained, suggesting that the proposed model is applicable for describing the chlorination kinetics of particles with low inner porosity.

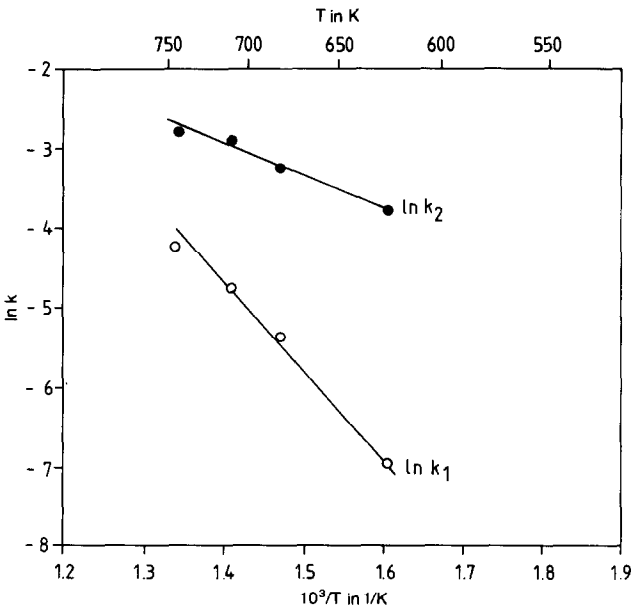

Fig. 6. Arrhenius representation of the rate constants obtained on the basis of the proposed kinetic model.

Figure 6 shows the temperature dependence of the rate constants (k_1 and k_2) used for the calculations. According to the expectations, an activation energy E_1 of 100 kJ mol^{-1} ($T = 620–740$ K) was obtained for the chemical reaction at the external surface. This value is in a good correspondence with that calculated from the initial reaction rates below 600 K. It can also be seen from Fig. 6 that the rate constant near the pore tunnels k_2 is higher than that of the interfacial chemical reaction; however, the slope of the corresponding Arrhenius plot is much lower due to the effect of the pore diffusion processes.

CONCLUSIONS

MO_3, as an acidic oxide, has a strong adsorption capacity towards the basic probe molecule, NH_3. There is no detectable interaction between SO_2 gas and the MO_3 surface. According to the microcalorimetric data, dissociative adsorption of NH_3 molecules with formation of Mo–NH_2 and Mo–OH species can be assumed.

On the basis of the kinetic and morphological results, the chlorination is controlled by the chemical processes below 600 K, while at higher temperatures the reaction becomes pore-diffusion-controlled. Activation energies of 110 and 53 kJ mol^{-1} with reaction orders of $n = 0.5$ and $n = 0.75$ were obtained in the temperature ranges 550–600 and 600–750 K, respectively. The dissociative adsorption of CCl_4 is assumed to precede the volatilization process.

Due to the extreme low porosity of the smaple, the reaction rate is different at the internal pore walls and at the external surface of the particles. In order to describe the conversion–time curves, a kinetic model is proposed involving both the reactions in a zone near the pore tunnels and at the external surface. The curves calculated with this model fit well to the experimental results.

ACKNOWLEDGEMENTS

This work was financed by the Hungarian OTKA Fund, project number: 3072.

REFERENCES

1 C.L. Rollinson, The Chemistry of Chromium, Molybdenum and Tungsten, Oxford, Pergamon Press, 1975.
2 M.L. Larson and F.W. Moore, Inorg. Chem., 3 (1964) 285.
3 M.L. Larson, Inorg. Synth., 12 (1970) 165.
4 W.W. Porterfield and S.Y. Tyree, Jr., Inorg. Synth., 9 (1967) 165.
5 D.E. Couch and A. Brenner, J. Res. Natl. Bur. Stand. Sect. A63 (1959) 165.
6 B.G. Ward and F.E. Stafford, Inorg. Chem., 7 (1968) 2569.
7 M.F. Kanunnikov, Zh. Prikl. Khim., 59 (1986) 1693.
8 M.F. Kanunnikov, Zh. Prikl. Khim., 60 (1987) 968.
9 M. Del Carmen Ruis, Lat. Am. Appl. Res., 20 (1990) 107.
10 A. Auroux and J.C. Vedrine, in B. Imelik, C. Nacache, G. Coudrier, Y. Bentaarit and F.C. Vedrine (Eds.) Catalysis by acids and bases. Stud. Surf. Sci. Catal., Elsevier, Amsterdam, 20 (1985) 311.
11 JANAF Thermochemical Tables, 2nd edn., Nat. Stand. Ref. Data Ser., National Bureau of Standards, Washington DC, 1971.
12 I. Barin and O. Knacke, Thermochemical Properties of Inorganic Substances, Springer Verlag, Berlin, 1973.
13 L. Kihlborg, The Crystal Chemistry of Molybdenum Oxides, Advances in Chemistry Series, Vol. 39, American Chemical Society, Washington, DC, 1963.
14 B. Pödör and I. Bertóti, Thermochim. Acta, 56 (1982) 209.
15 J.H. Sharp, G.W. Brindley and B.N. Achar, J. Am. Ceram. Soc., 49 (1966) 379.
16 P.L. Walker, Jr., F.F. Rusinko, Jr, and L.G. Austin, Adv. Catal., 11 (1959) 133.
17 J. Szekely, J.W. Evans and H.Y. Song, Gas–Solid Reactions, Academic Press, New York, 1976.